

Acoustic Emission for Diagnosis of Train Rotating Systems

Professor Dr Andy Tan

Chairman – Centre for Railway Infrastructure and Engineering

LKC Faculty of Engineering and Science

Universiti Tunku Abdul Rahman

Sungai Long, Cheras, 43000 Kajang

Selangor, Malaysia

- Part 1- Introduction to Railway in Malaysia
- Part 2- Acoustic Emission for diagnosis of train rotating system



Headquarters of the F.M.S. Railways at Kuala Lumpur - circa 1910.

The History of KTM Railway

1885

The first railroad in Malaya which links Taiping to Port Weld (Kuala Sepetang) open by Sir Hugh Low.



1866

Route between Kuala Lumpur and Port Klang opened



1891

Track connecting Seremban and Port Dickson opened

1893

Track connecting Teluk Anson and Tapah Road opened

1896

Establishment of Federal Malay States Railway



1900

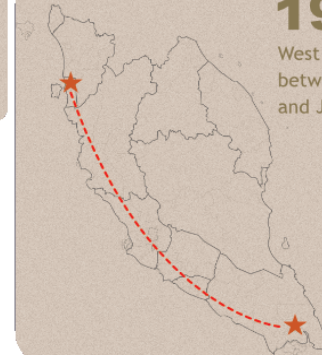
Victoria Railway Bridge opened

1903

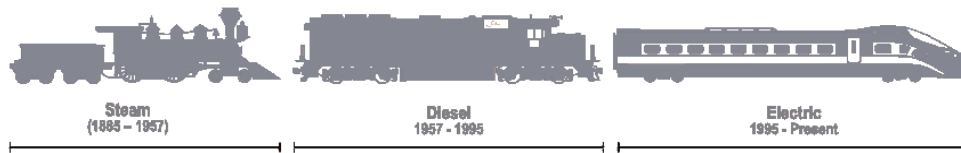
Track between Tank Road and Woodland (Singapore) opened for service

1909

West Coast rail track between Prai (Penang) and Johor Bharu opened



KTMB TRANSFORMATION



1931

East coast rail link track between Tumpat and Gemas opened . Gua Musang and Kuala Gris become the last sector at that time

1995

The first KTMB electric commuter started operation in Malaysia. Covering central Region (Port Klang Line & Seremban Line)



2014

Ipoh - Padang Besar double track began operation



2015

First KTM ETS (Electric Train Service) began its operation connecting KL Sentral - Padang Besar and Padang Besar to Gemas



2015

KTM Komuter North Region and Shuttle Tebrau (JB - Woodland) started operation



2018

Subang Skypark Komuter began its operation connecting KL Sentral - Subang Terminal Airport



2018

Electronic ticket purchasing using mobile technology (Android & IOS) introduced



Diesel trains

Based on 1m guage with total distance of the network at 1,699 km.

Launch its first diesel engine, a Class 15 Shutter, in 1948 and fully convert to diesel power between the 1950s and 1970s, and till recently.



Class 29 diesel locomotive at Gemas Railway Station (Sept. 2009), Dalian Locomotive

Electric Trains

Electric trains were only introduced in 1995



*Electric locomotive Škoda
ChS4-109*

Recent KTM Inter-city Trains

The KTM West Coast Line between Singapore and Padang Besar, on to the Malaysian-Thai border.



The KTM East Coast Line between Gemas in Negri Sembilan and Tumpat in Kelantan and branches between Kuala Lumpur, Port Klang, and other cities in peninsular Malaysia.



Express Rail Link (ERL)

Operate between Kuala Lumpur and International Airport KLIA and KLIA2. Maximum speed is about 160 km/h (99 mph) and distance of 57 km.

Operate in 14 April 2002 with a ridership of 6.6 M passenger in 2017



Rolling – 4x4 CRRC Changchun Articulated EMU and 4x4 Desiro ET 425 M Articulated EMU

Light Rapid Transit (LRT)

The three light rapid transit lines in Kuala Lumpur are the Kelana Jaya Line, the Ampang Line and Sri Petaling Line.

The line was completely opened in 1998.



Kelana Jaya line

The Kelana Jaya Line is a driverless automatic system and is 46.4 km (29 mi) long, running between the northeastern suburbs of Kuala Lumpur and Petaling Jaya to the west of Kuala Lumpur. Started operation 1999.

Servicing 37 stations, running mostly on underground and elevated guideways. Fully automated Driverless



*Bombardier Innovia Metro
300 train*

Ampang and Sri Petaling lines

The third and fourth rapid transit lines in Klang Valley. The combined network comprises 45.1 kilometres of track (28 miles) with 36 stations, and is the first to use the standard gauge track and semi-automated trains in Klang Valley.



6-car CSR Zhuzhou Amy Articulated LRV

Mass Rapid Transit (MRT)

Phase 1 (Sungai Buloh - Kajang) started its operation in 15 December 2016. 47 km in distance serving a population of 1.2M people in the region. Ridership in 2017 – 2.25M
Construction cost estimated MYR36 billion



A Siemens Inspiro EMU stock

KL – Singapore HSR

- Feasibility studies in 2006 and as of June 2007, the project cost RM8 billion project would slash travel time from more than 6 hours to about 90 minutes.
- The main stumbling blocks, apart from costs, appears to be the JB-Woodlands Causeway.
- On January 2008, the government is still looking in the proposal and had yet to make a final decision.
- On 22 April 2008, the government announce that the project was put on hold indefinitely due to high cost.
- On March 2009, to revive the project again, it will seek to build the rail line on the coastline on the existing track.
- In September 2010, Malaysia and Singapore formalized the construction of HSR, officially agreed in February 2013 to go ahead and set a completion date of 2026.
- In May 2018, the newly-minted Prime Minister announced the cancellation of the project and will resume in Jan 2031.

Original time-line

This was the planned timeline. However, the project was postponed by the Malaysian Government.

- **19 July 2016:** Signing of MOU for KL–Singapore HSR project
- **August 2016:** Singapore to call tender for advance engineering studies. Singapore–Malaysia joint tender for Joint Development Partner
- **13 December 2016:** Bilateral agreement signed
- **Late 2017:** Civil works and tender for private entity overseeing train and rail assets
- **2018–2025:** Construction
- **Late 2023:** International and domestic operators tender
- **2024–2026:** Testing and commissioning
- **By December 31, 2026:** Operation

Japan's high speed bullet trains, Shinkansen trains, has a top speed reaching up to 320 km/hr



*Chinese designed
CRH380AL train*



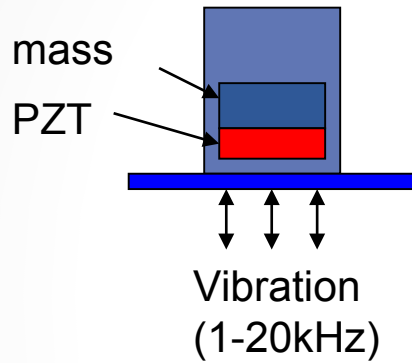
Motivation

- The benefits and challenges of AE for fault detection
- Peak Hold Down Sampling to resolve massive data storage due to high sampling frequency
- Normalization of signal response of different AE sensors in multi-sensor application
- Case study on diesel engine
- Case study on mixer gearbox

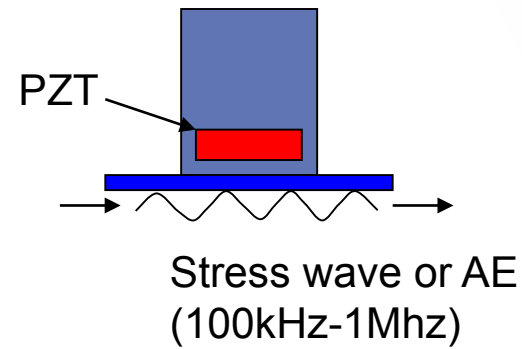


Vibration vs. AE

Accelerometer

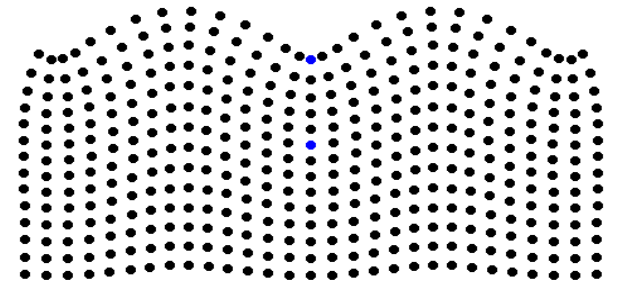
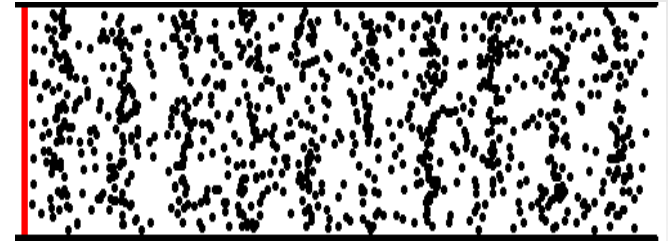


AE sensor



Acoustic Emissions

- Acoustic emissions are **transient elastic waves generated by the rapid release of energy from localized sources** within and on the surface of a material (up to 1MHz)
- Sources: crack initiation/propagation, friction, rubbing, impacting, turbulent flow
- Main benefits : high S/N ratio, crack detection, early detection of mechanical integrity
- Challenges : where multiple AE sources exist, global monitoring, hardware implementation
- Applications : cracks in structure (bridge, vessel, tank, pipeline etc.), bearings, seals, gearbox, diesel engines, leak detection, low speed machine



©1999, Daniel R. Russell

Piezoceramic Sensor and Actuator

1. Actuator – Induced Moment

$$M(T) = -V(x, t)d_{31}(T)\left(\frac{t_b + t_p}{2}\right)\left(\frac{E_b(T)t_b E_p(T)W_p}{E_b(T)t_b + E_p(T)t_p}\right)$$

2. Sensor – Voltage Generated

$$v_s(t) = k_s[y'(t, x_2) - y'(t, x_1)]$$

Sensing Constant $k_s = \frac{g_{31}E_p z_c W_p^2 L_p}{t_p}$

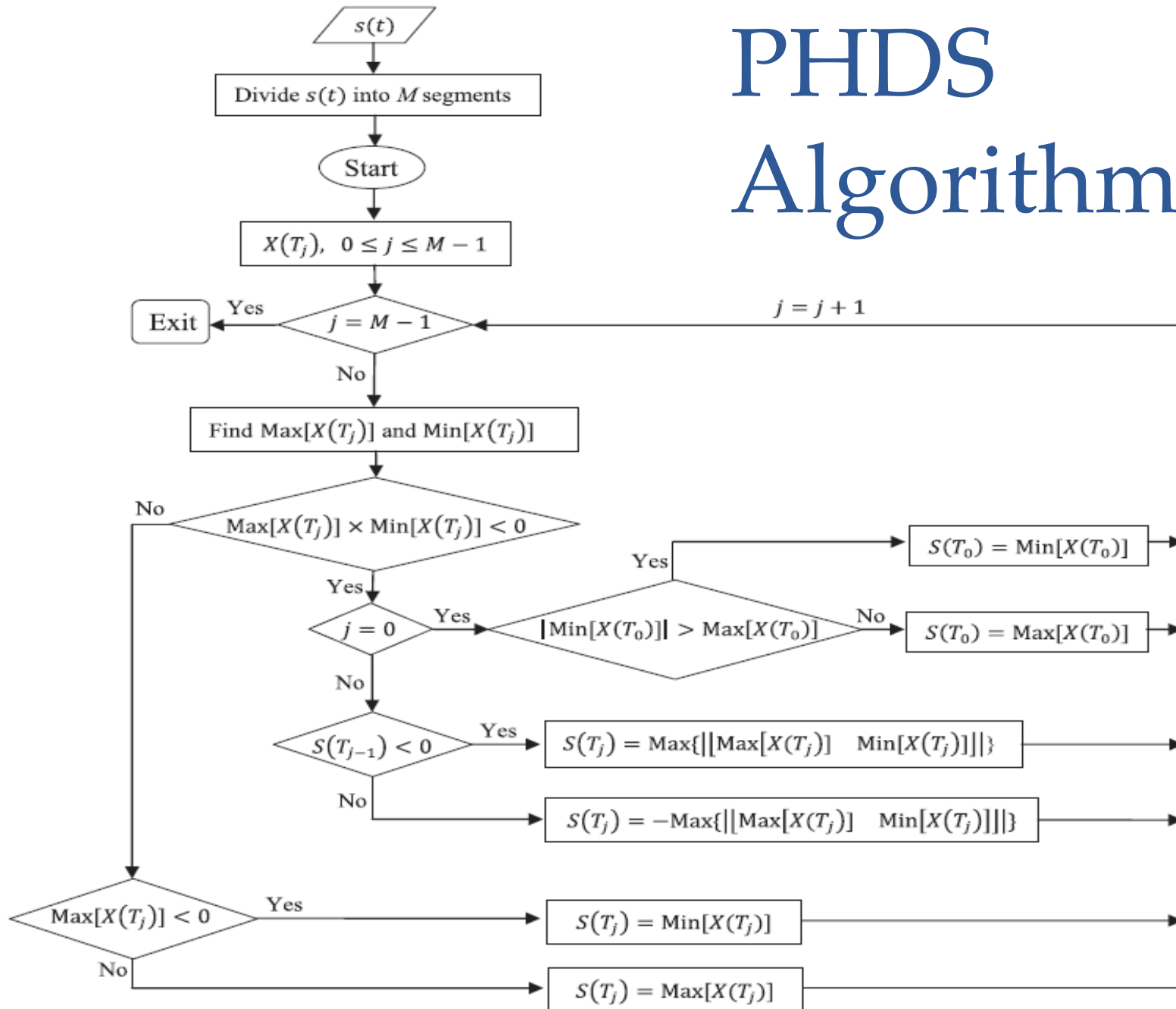
Peak Hold Down Sampling

Peak Hold Down Sampling

- Due to low rotating speed and to capture sufficient data for a few complete shaft rotations will end up with massive data storage at high sampling rate.
- Transmission of large amount of data for storage and analysis from remote sites will require massive data transfer and limitation of current technology.
- Traditional down sampling selects every i th sample at equal intervals and discard the rest of the data from the original data to reduce the data size and result in loss of vital information.
- Peak-Hold-Down-Sampling (PHDS) retains critical impulses due to bearing and gearbox defects in the time waveform.



PHDS Algorithm



Mathematical Description

$s(t) = [s(t_0), s(t_1), s(t_2), \dots, s(t_i), \dots]$, $0 \leq i \leq N-1$, can be written as:

$$S(T) = [S(T_0), S(T_1), S(T_2), \dots, S(T_j), \dots], \quad 0 \leq j \leq M-1,$$

where $M = \text{int}(N/r)$ and $r = f_o/f_d$ is the down-sample ratio.

$f_o = 1/(t_{i+1} - t_i)$ is the sampling frequency of the original data

$f_d = 1/(T_{j+1} - T_j)$ is the sampling frequency of the down-sampled data series

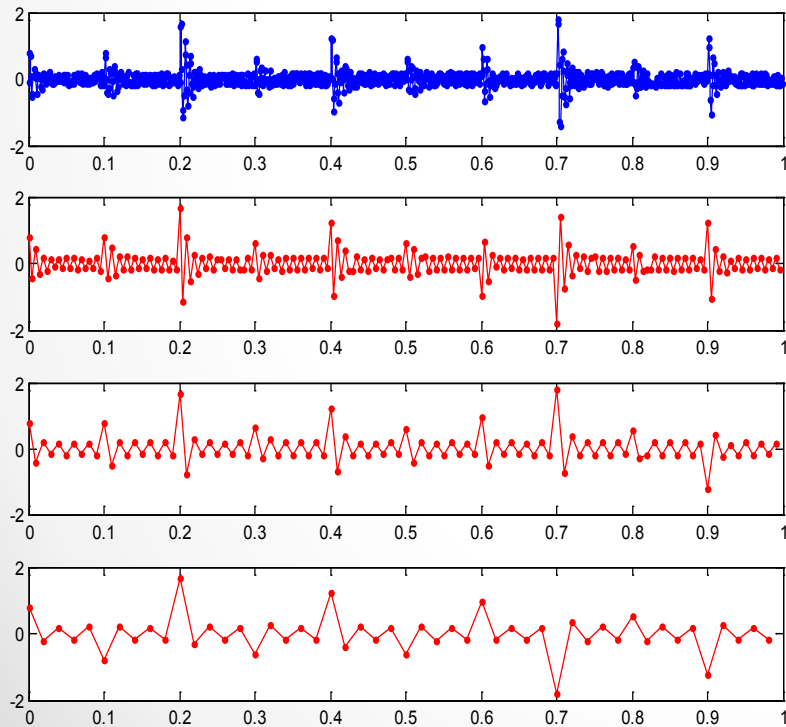
The data segment $X(T_j)$ described in Fig. 1 is given by

$$X(T_j) = [s(t_i), s(t_{i+1}), s(t_{i+2}), \dots, s(t_{i+r})], \quad \text{where } t_i \geq T_j \text{ and } t_{i+r} < T_{j+1}.$$

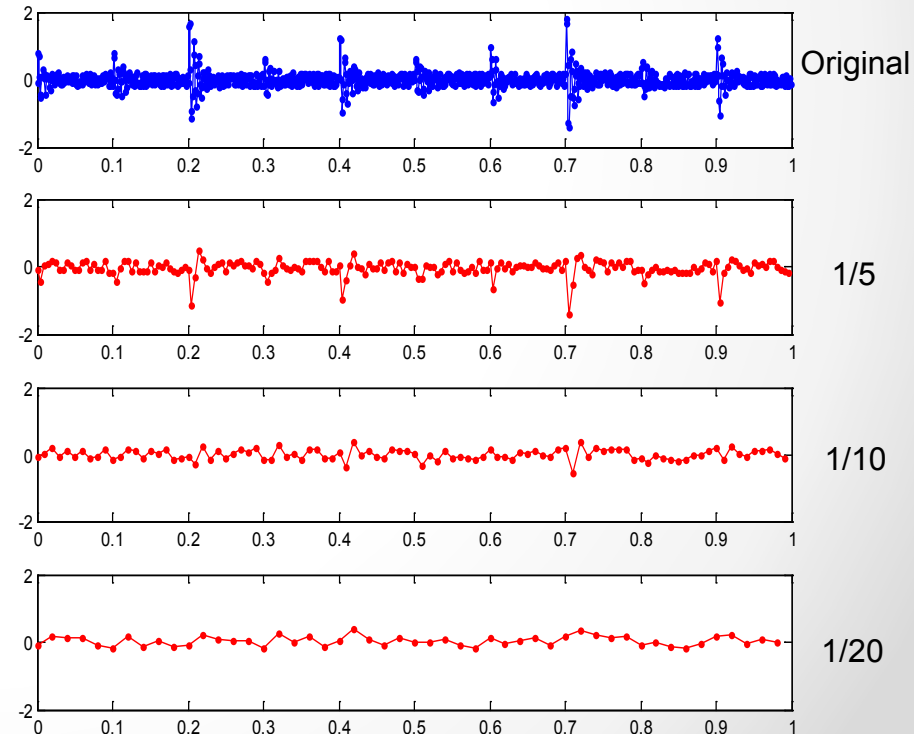
Peak Hold Down Sampling

- Main challenges in AE application to low speed machinery → huge amount of data → missing frequency information
- Peak Hold Down Sampling :
 - Detects high frequency impact information with very slow speed sampling

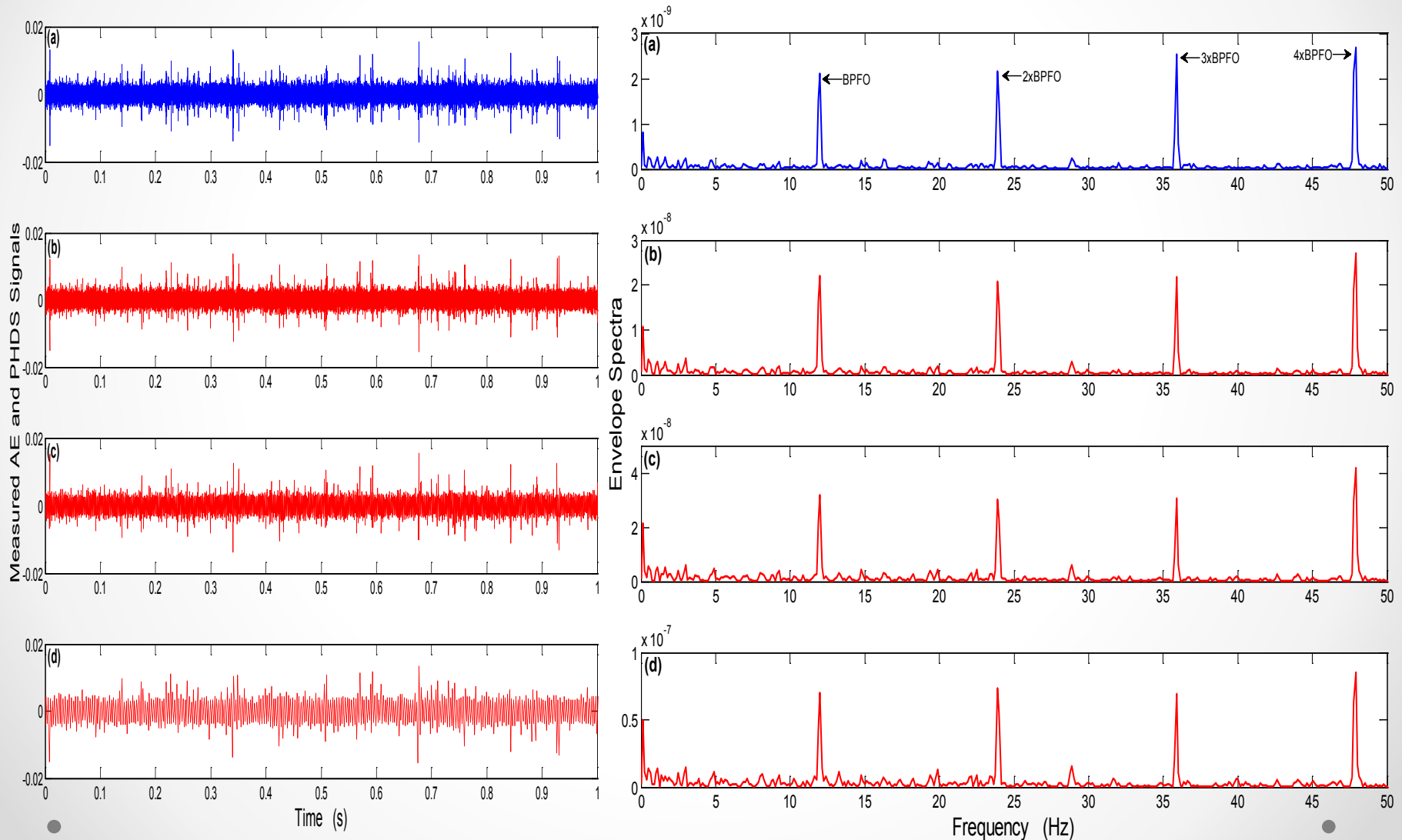
Peak Hold Down Sampling



Normal Down Sampling



(a) Original acoustic emission signal sampling at 131 kHz;
(b) PHDS signal sampling at 2.62 kHz; (c) Sampling at 1.31 kHz;
and (d) Sampling at 524 Hz.



Case Study 1

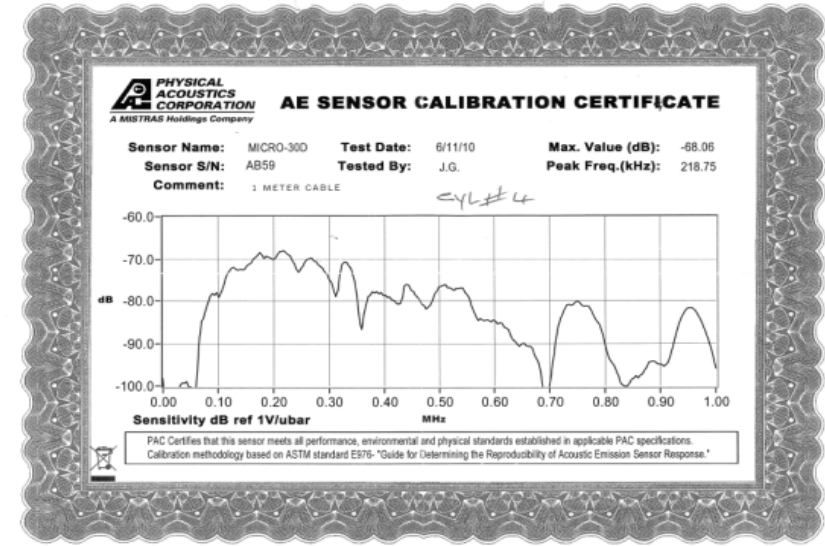
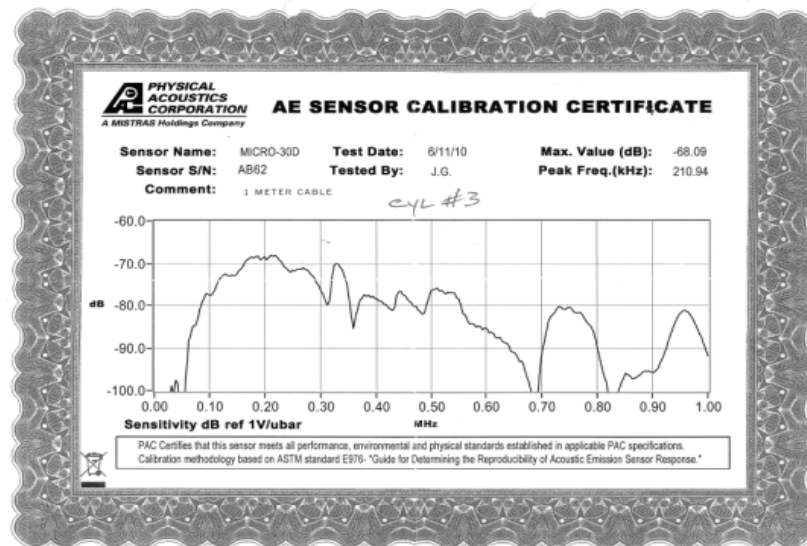
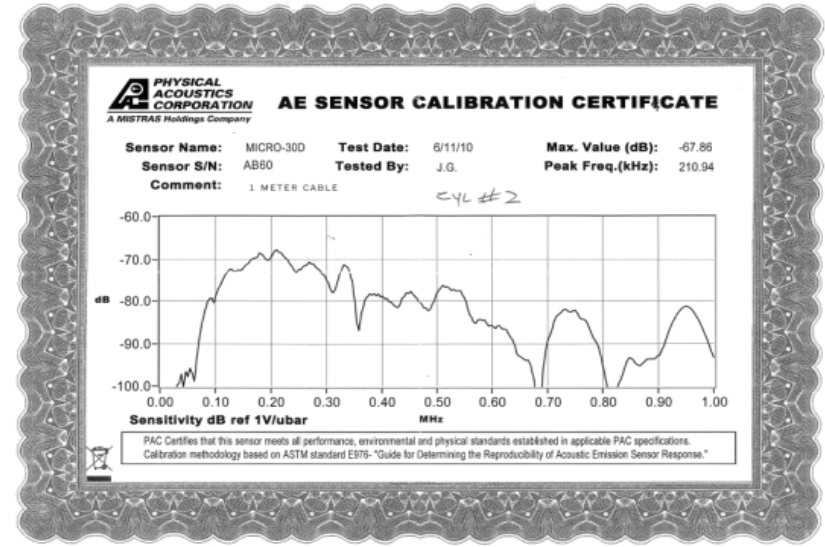
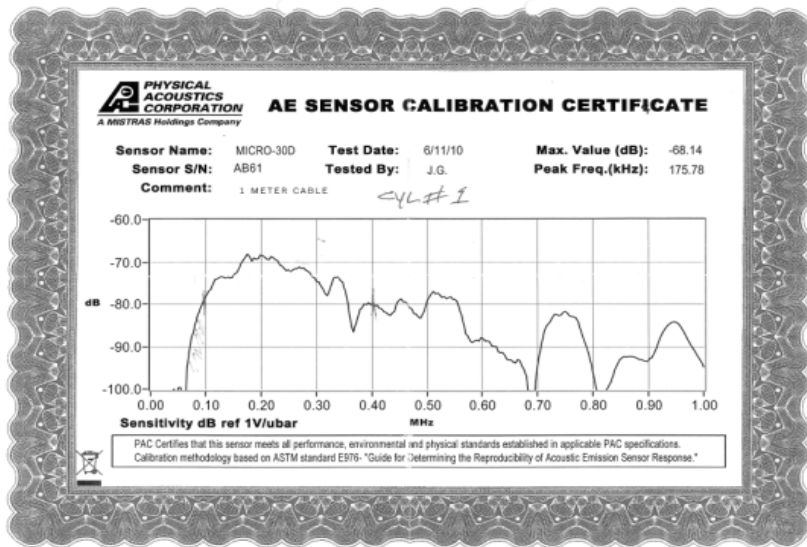
Normalization of output response AE Sensors

The benefits of signal normalization

- (1) It overcomes the inherent nonlinear response problem of AE sensors
- (2) It normalizes the AE response to enable a direct comparison as well as quantitatively analyze the AE signals measured by different sensors in the time domain
- (3) The AE signals after normalization can be displayed directly in the true physical unit rather than in arbitrary units or signal voltage



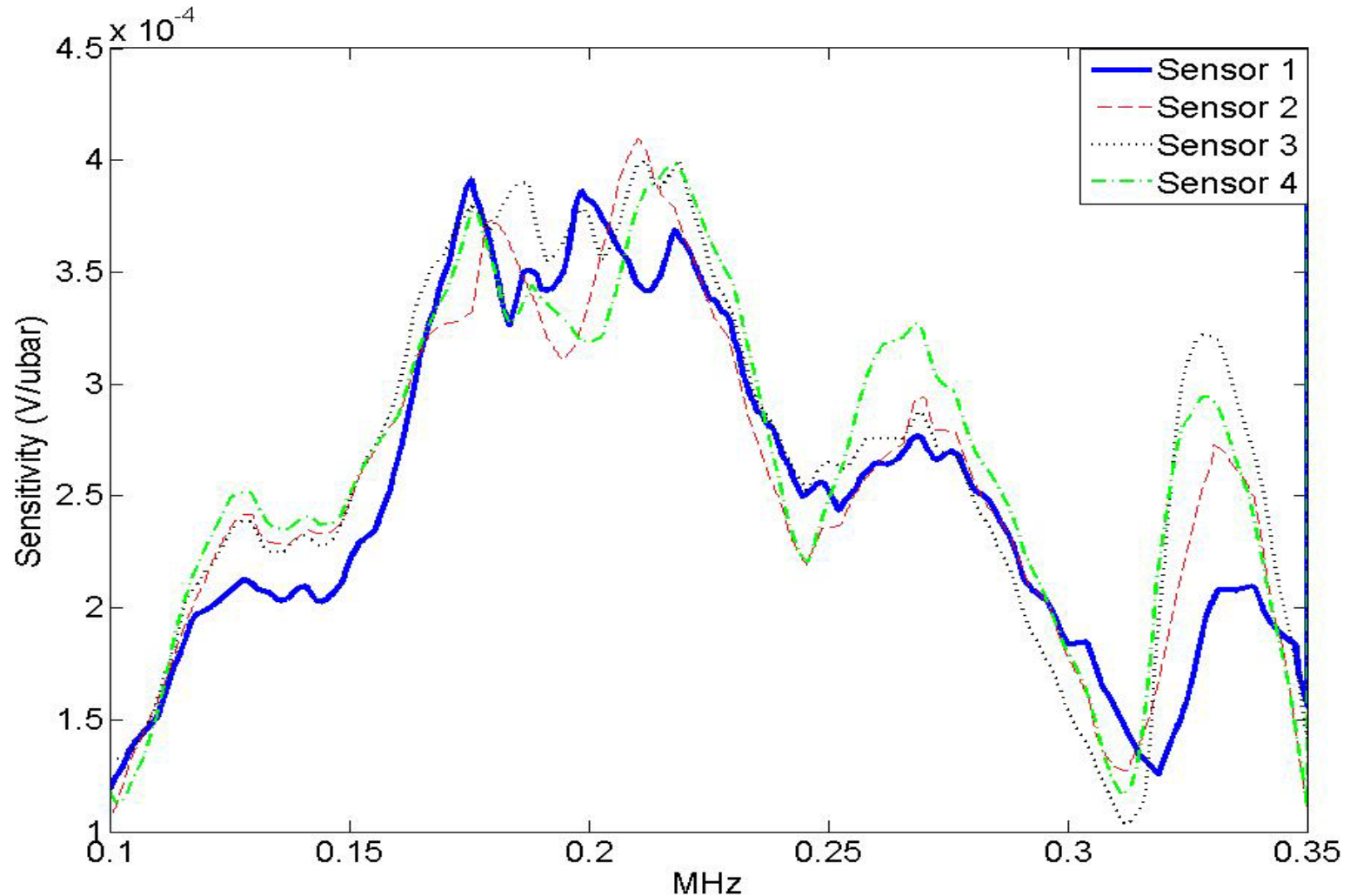
The calibration charts of AE sensors



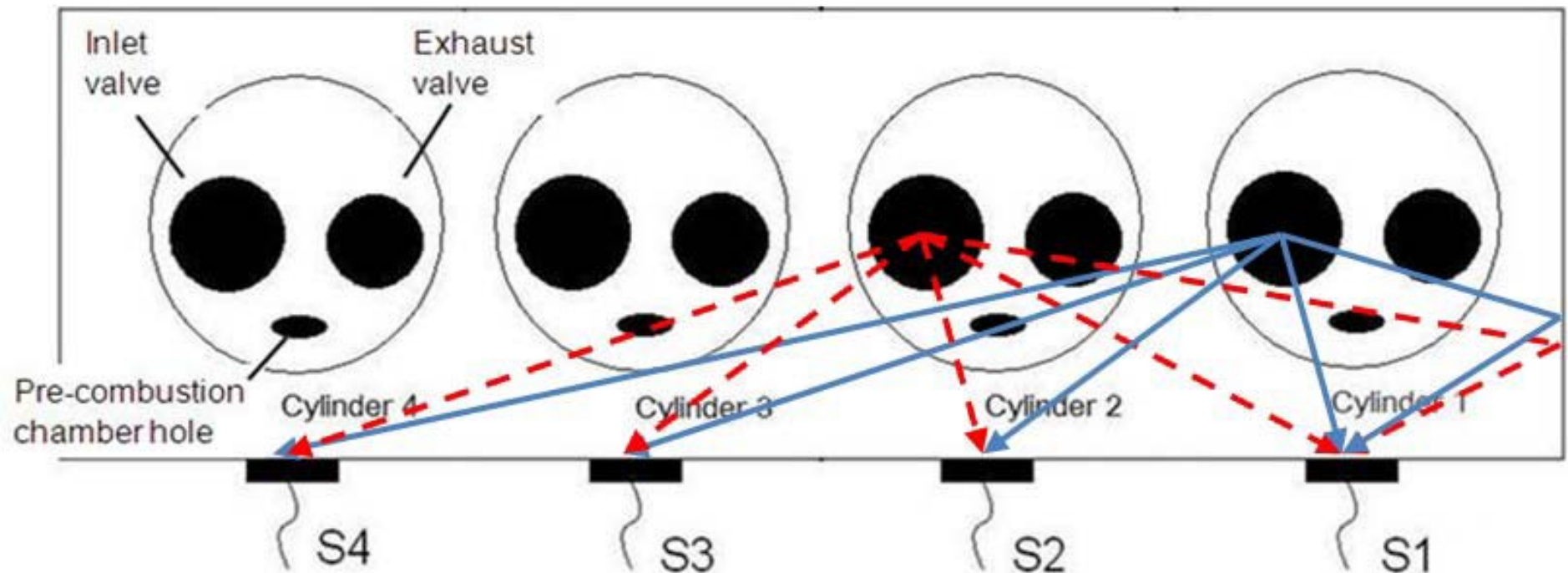
Procedure

- The calibration chart of each sensor was scanned and digitalized at a frequency interval of 0.01 MHz
- The original dB scale of the calibration charts converted into the linear scale
- Sensitivity of AE sensor displayed in the linear scale

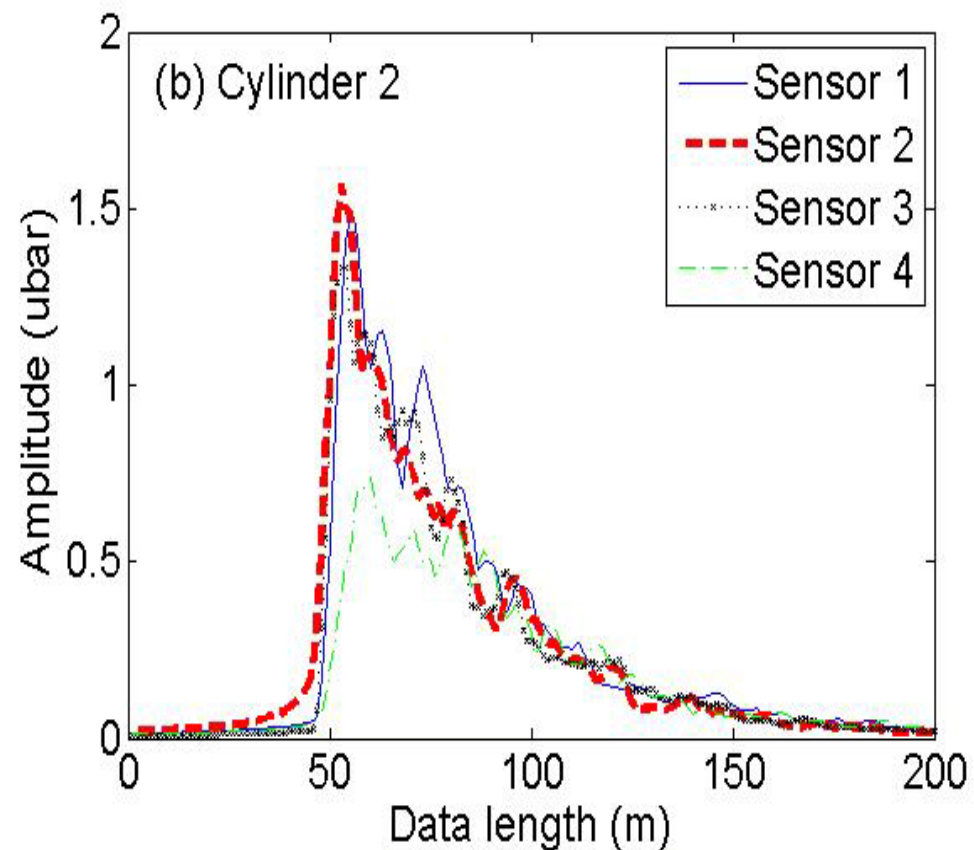
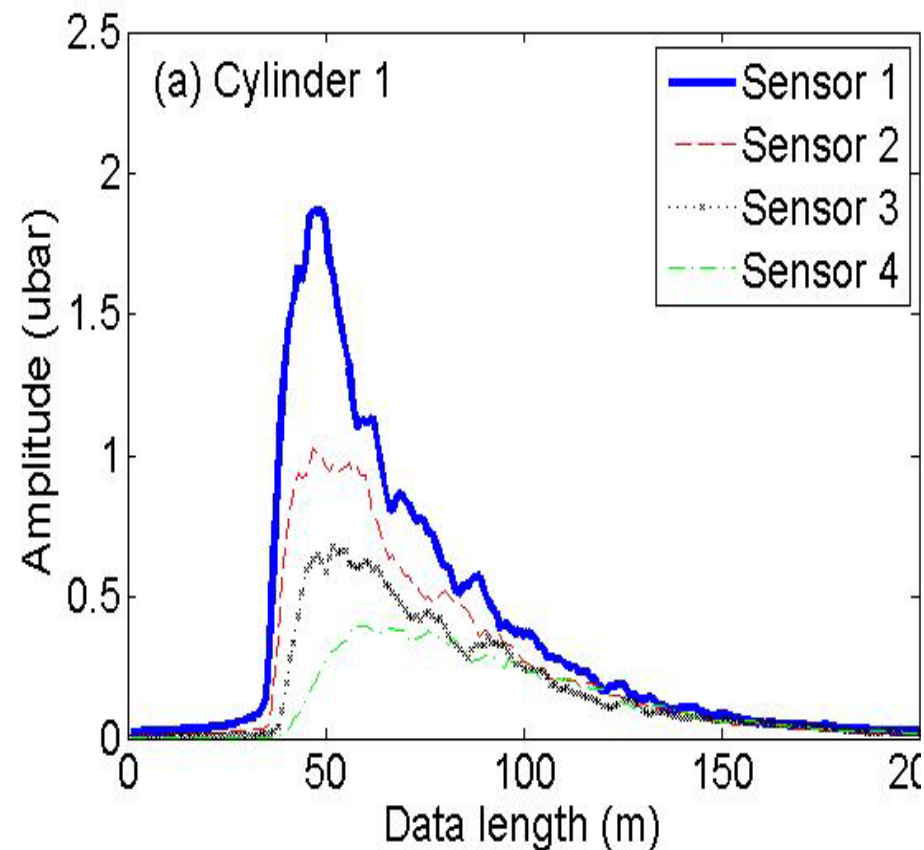
Digitized calibration charts of AE sensors



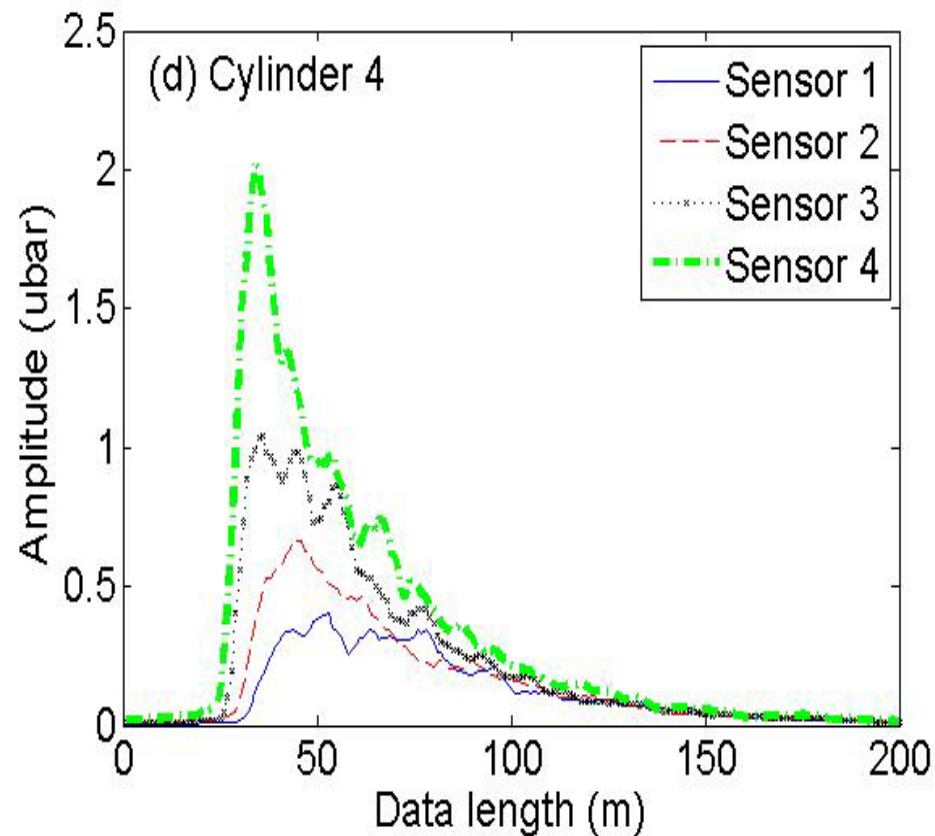
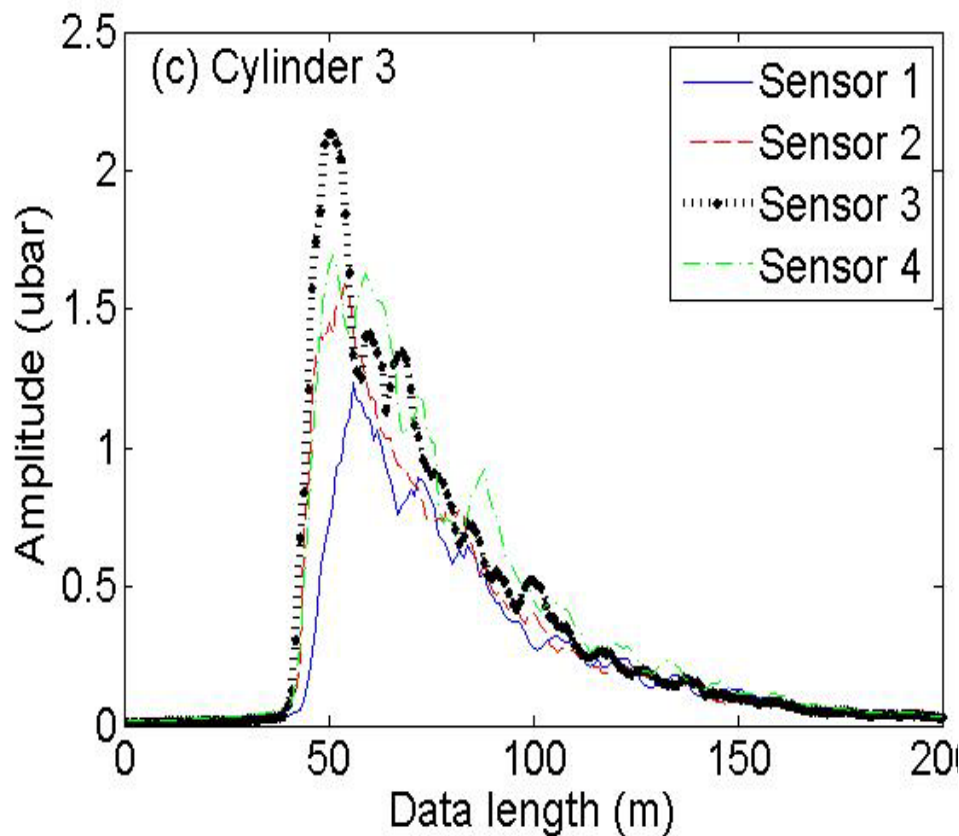
PLB test and system parameters determination



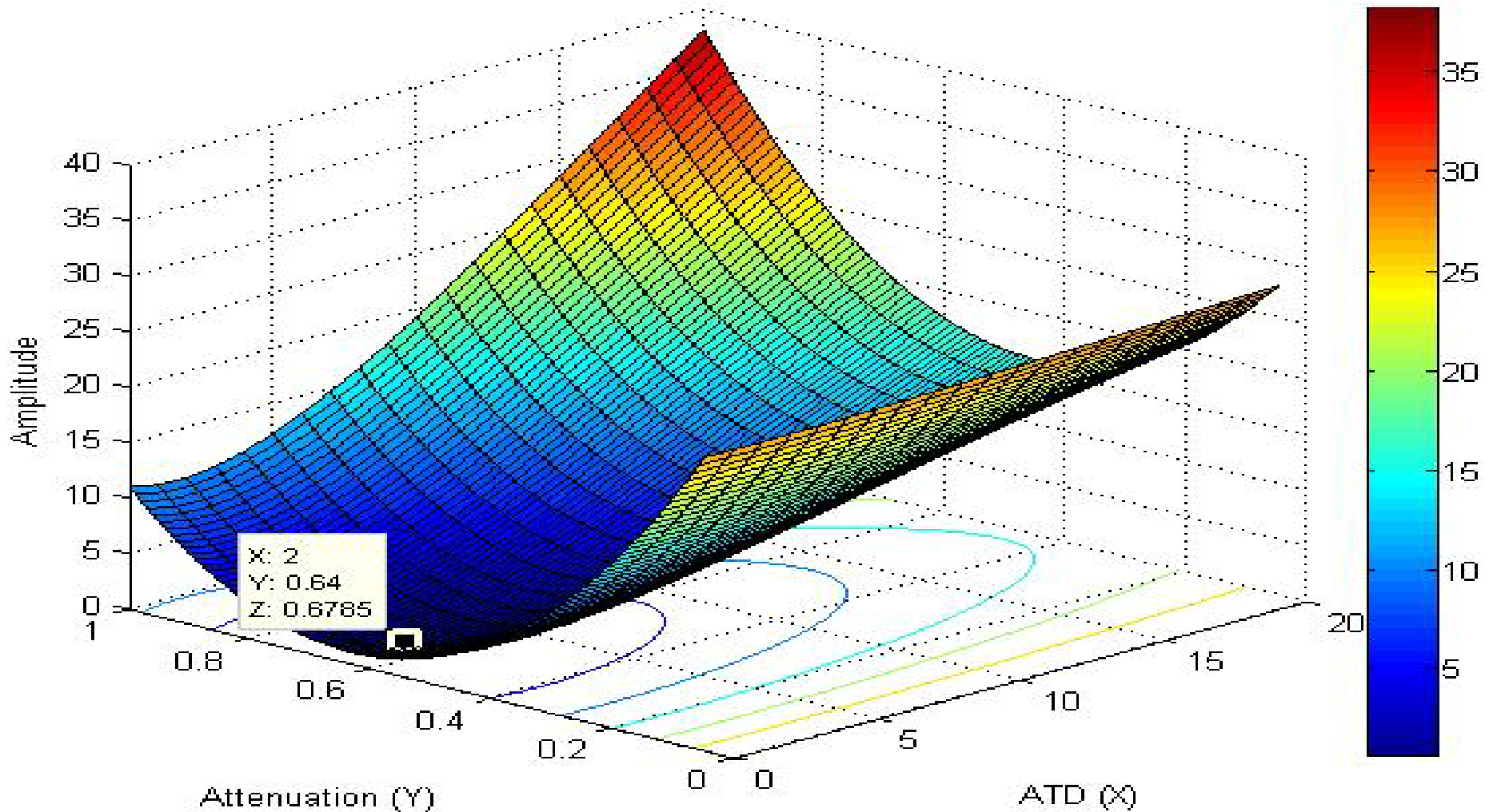
Averaged AEE responses of the PLB test at each cylinder



Averaged AEE responses of the PLB test at each cylinder



3D plot of evaluating the optimized attenuation and ATD parameters



Attenuation constant matrix and ATD matrix for the test engine, α and β

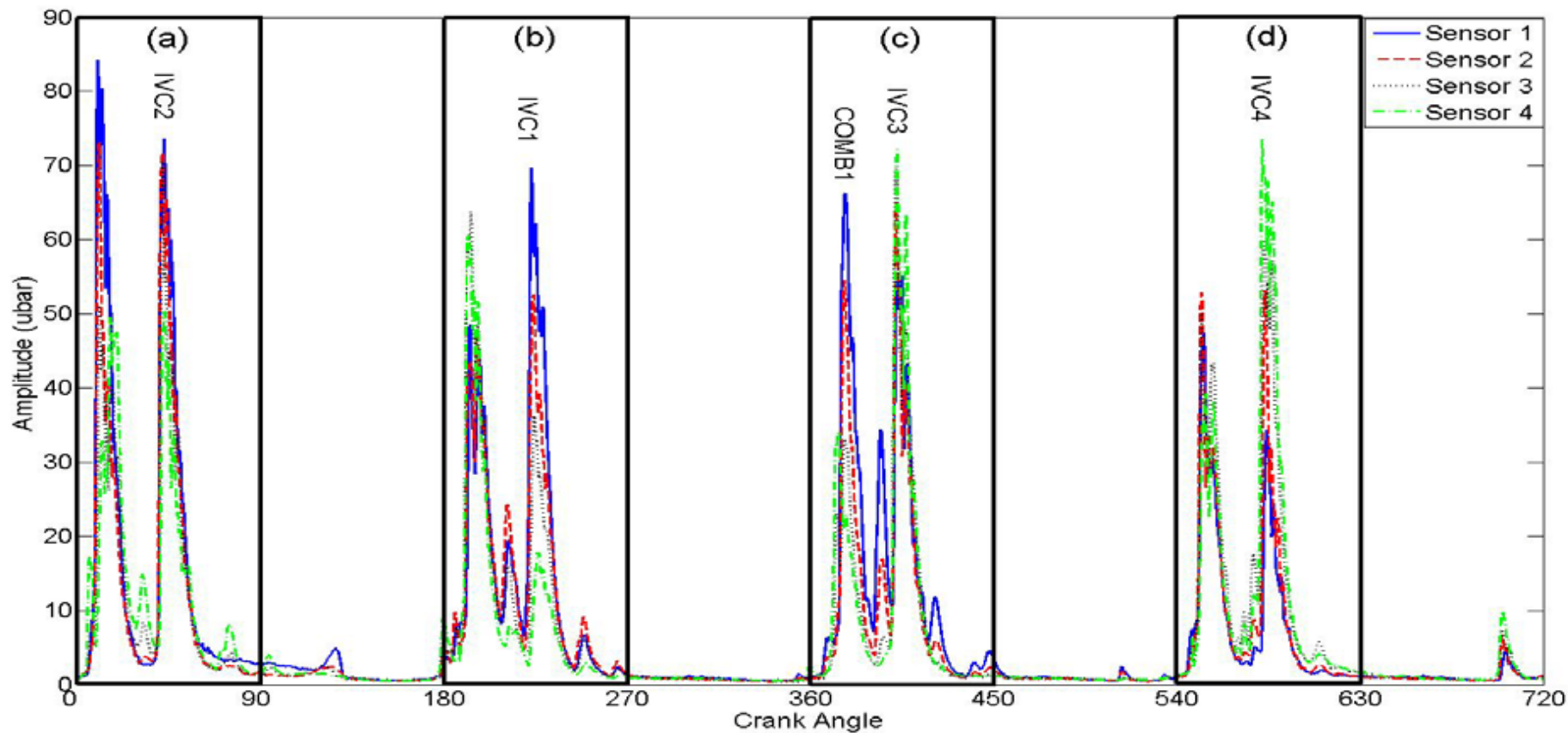
$$\alpha = \begin{bmatrix} 1 & 1 & 0.63 & 0.28 \\ 0.64 & 1 & 0.81 & 0.41 \\ 0.44 & 0.95 & 1 & 0.66 \\ 0.29 & 0.62 & 0.94 & 1 \end{bmatrix},$$

and

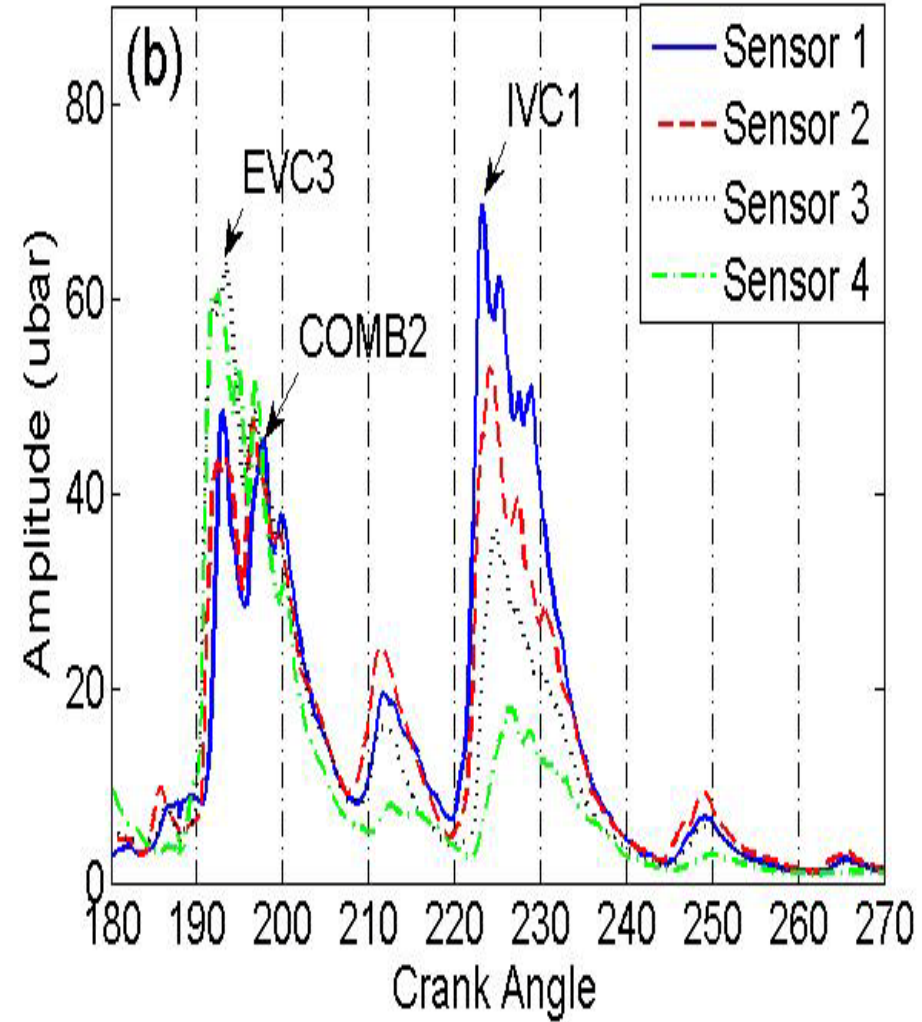
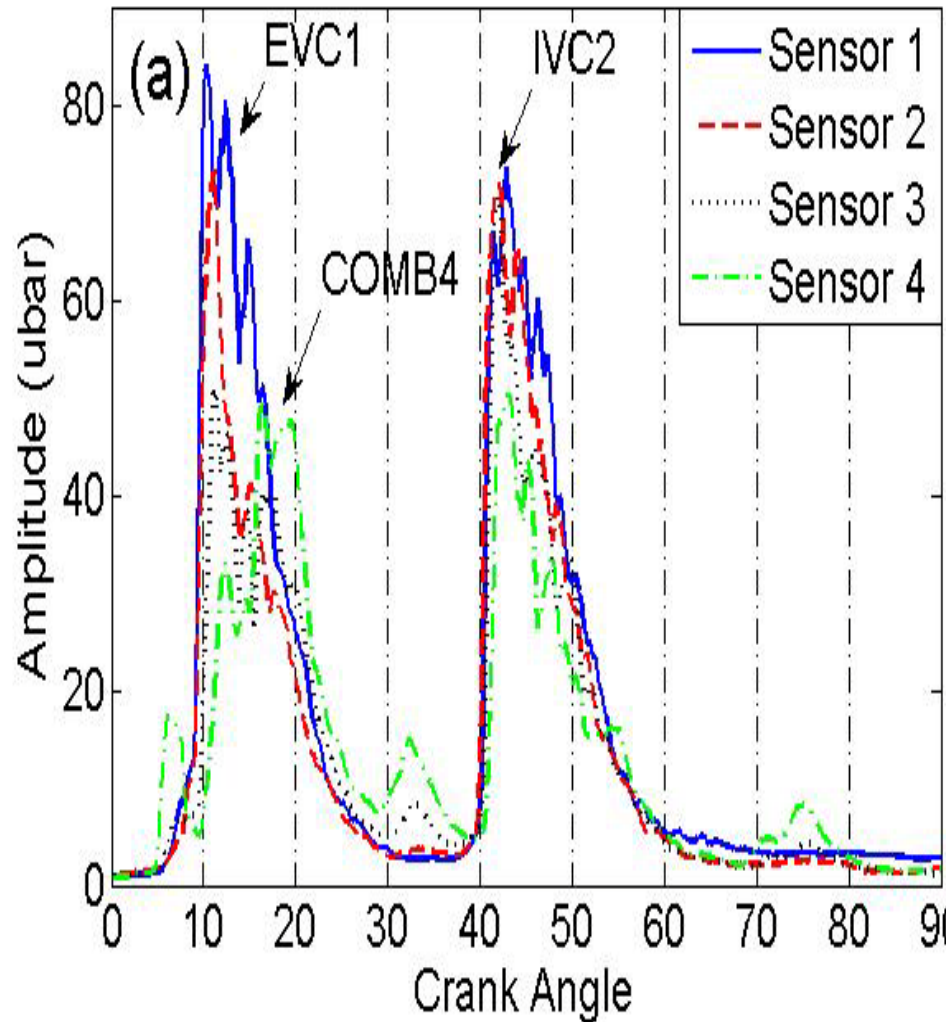
$$\beta = \begin{bmatrix} 0 & 2 & 6 & 11 \\ 2 & 0 & 1 & 7 \\ 5 & 0 & 0 & 2 \\ 13 & 5 & 1 & 0 \end{bmatrix},$$

An Example of AE signal

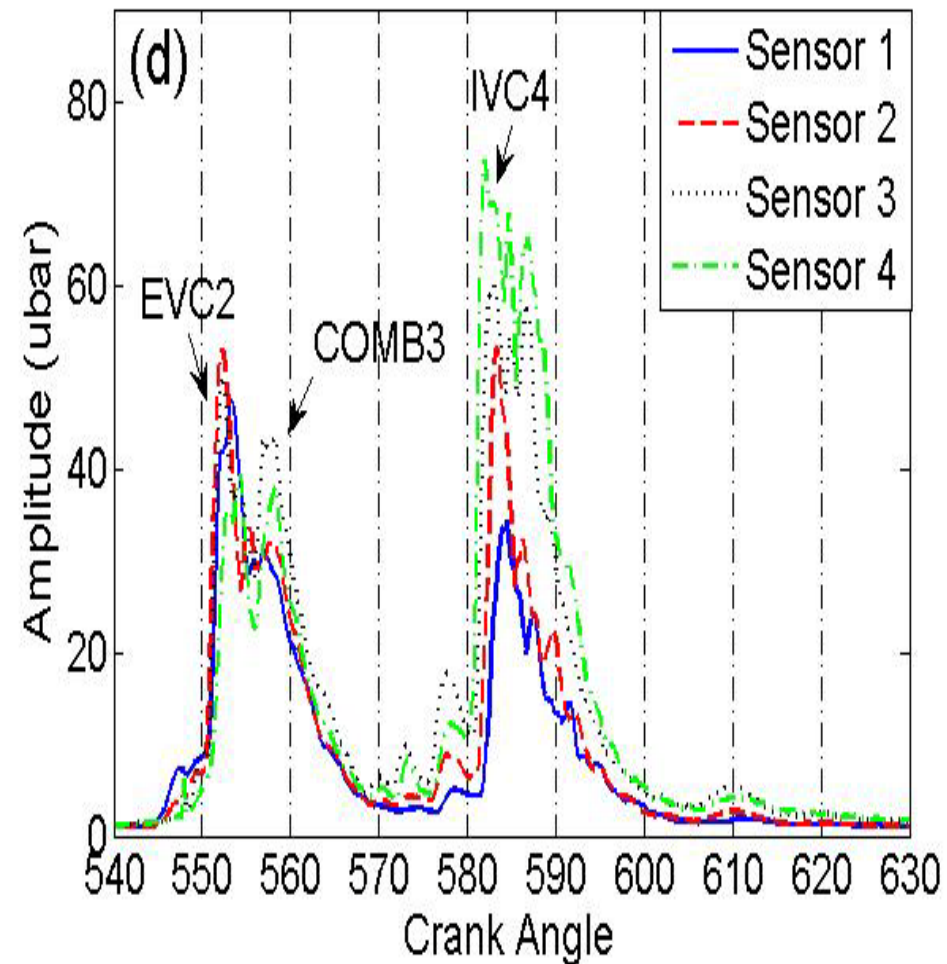
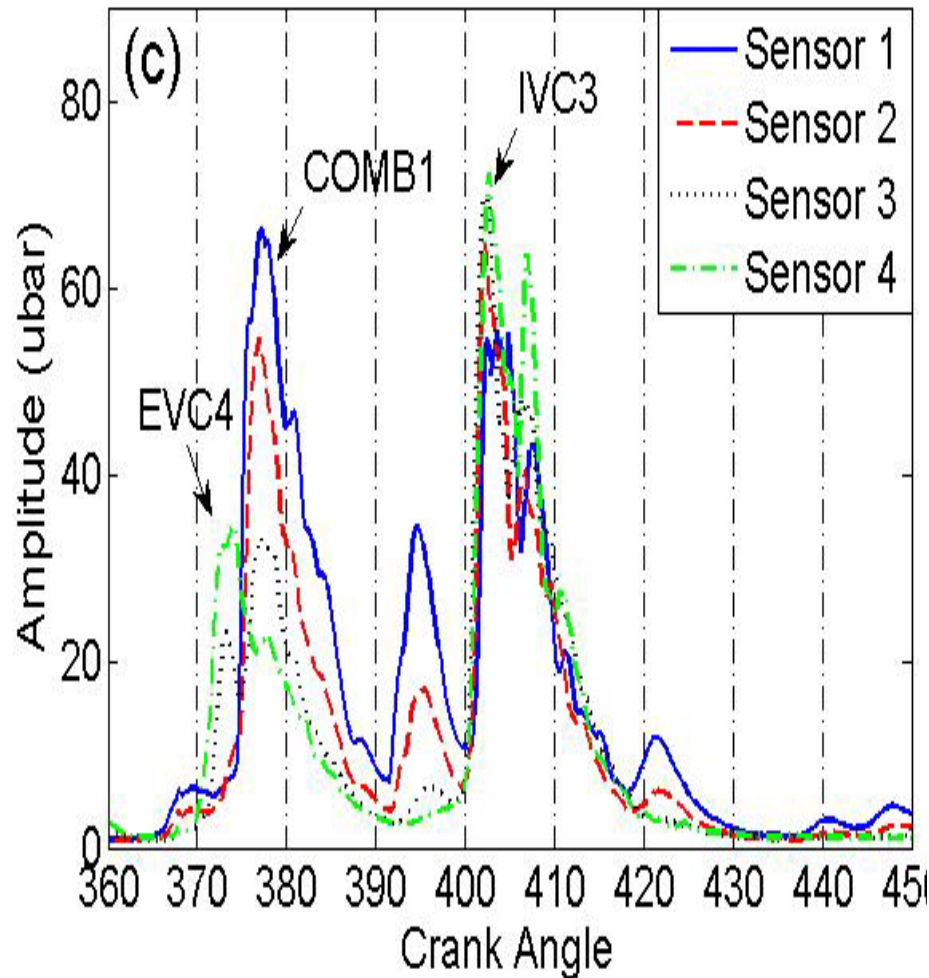
Normalisation of Diesel Engine



Enlarged view of the combustion areas

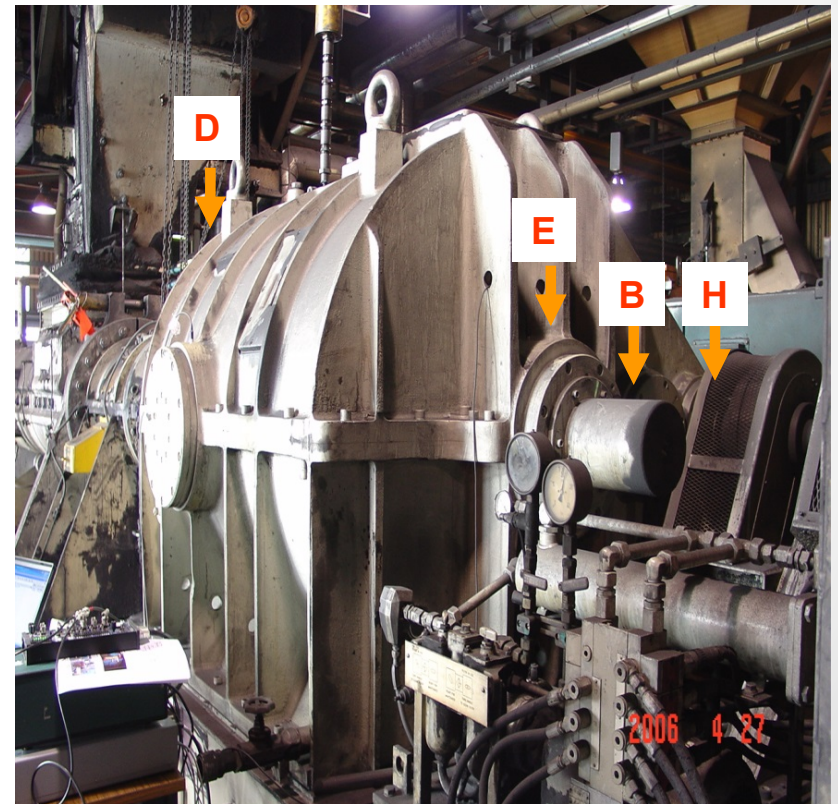
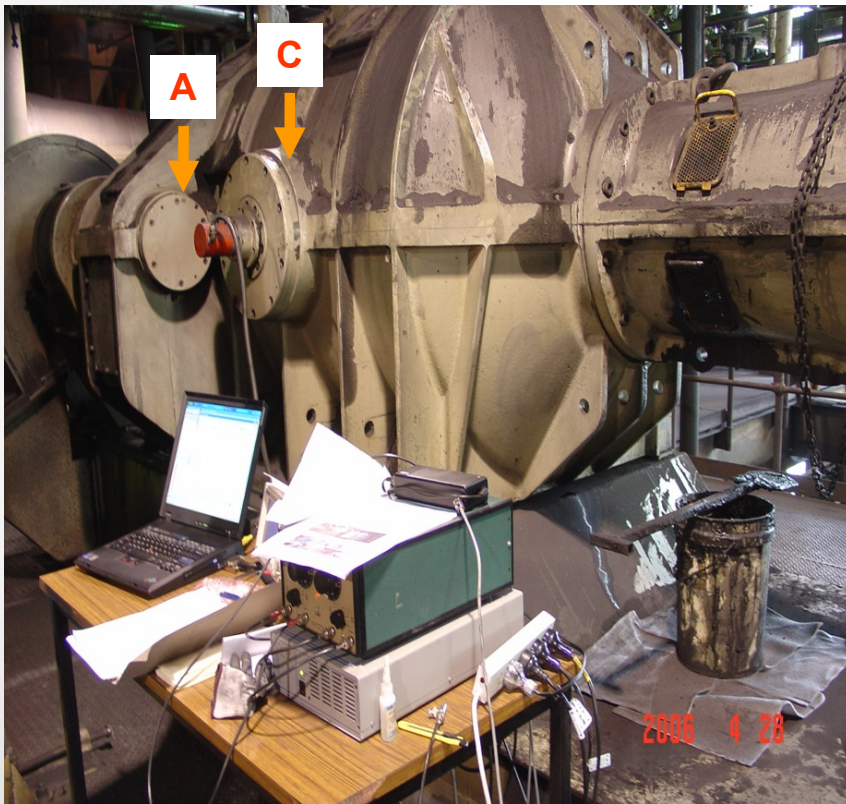


Enlarged view of the combustion areas



Case study 2

Green carbon mixer gearbox

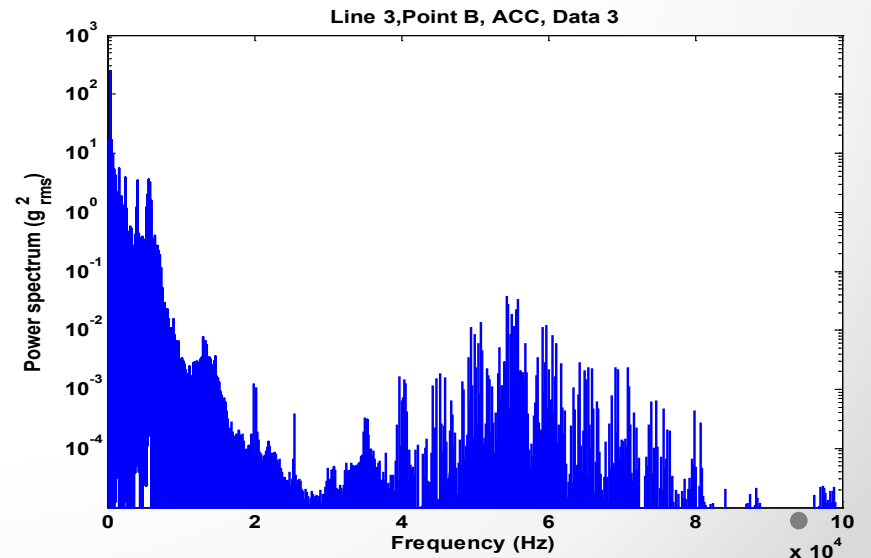
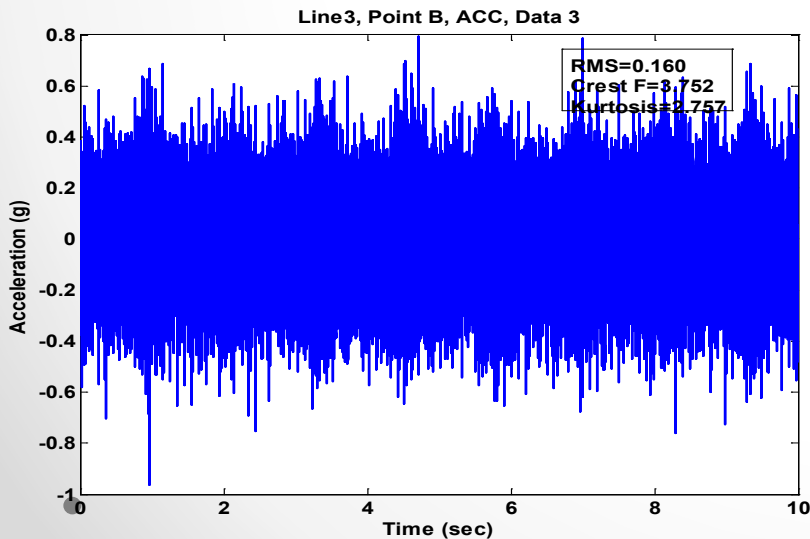
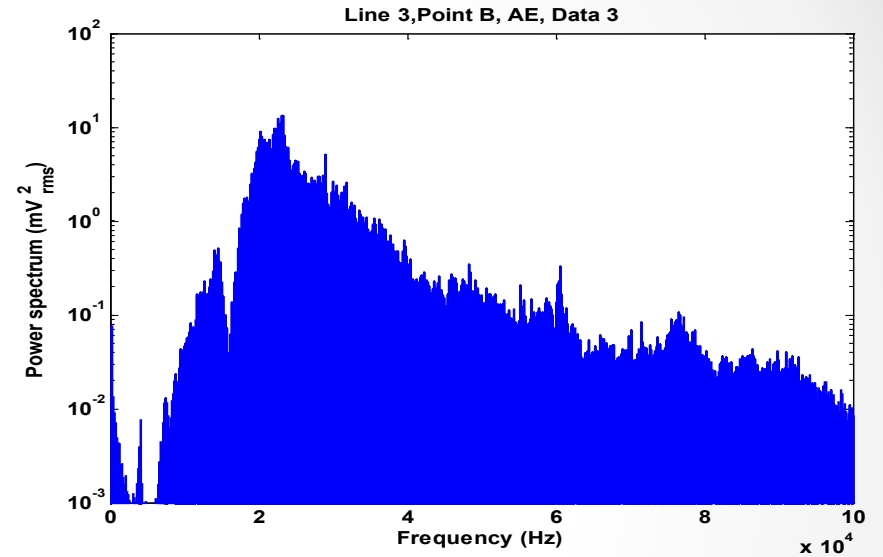
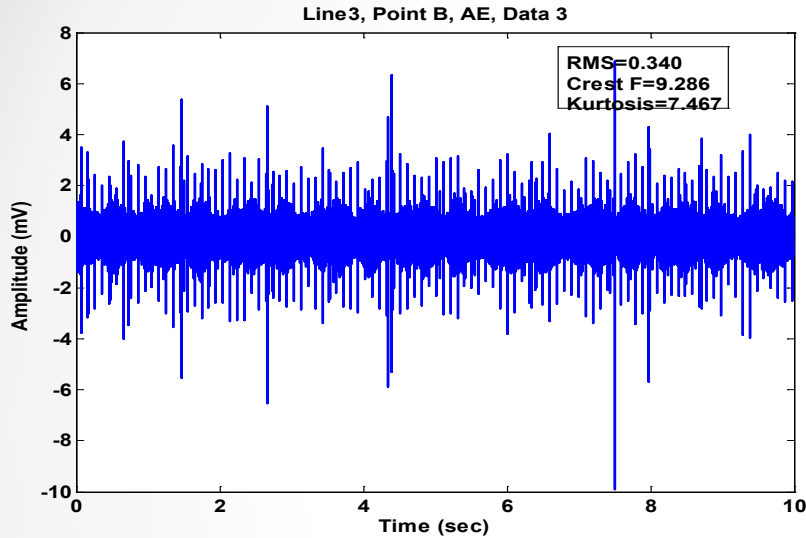


Bearing designations and defect frequencies

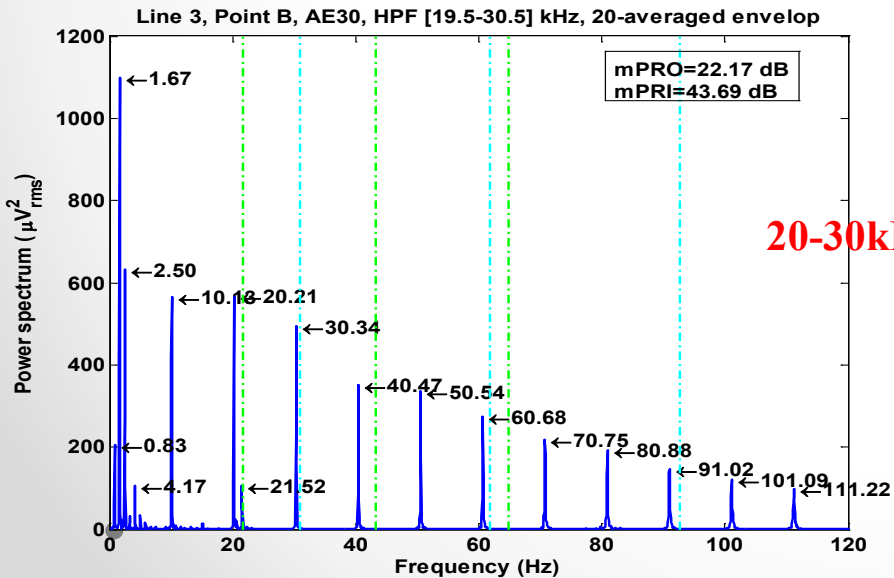
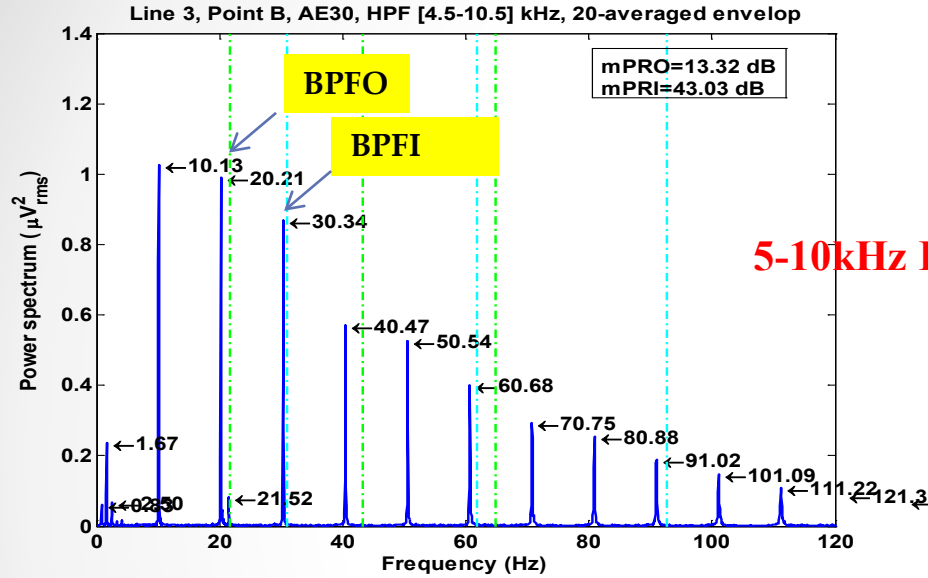
No.		Speeds (rpm)	Bearing defect frequencies (Hz)			
			BPFI	BPFO	BSF*2	FTF
1A	22320E	735	115.27	80.73	65.54	5.05
2H	22322E		115.52	80.48	64.80	5.03
3	23226CC/WW33	210	37.80	28.77	24.96	1.52
4B	22324CC/WW33		30.91	21.60	18.59	1.44
5,7E	23048CC/WW33	50	12.33	10.17	8.42	0.38
6	QJ1040N2MA		9.67	7.82	6.30	0.37
8CD	22326CC/WW33	50	7.35	5.15	4.46	0.34
9	22334CC/WW33		7.34	5.16	4.52	0.34
10	22230CC/WW33	50	9.00	6.81	5.78	0.36
11	29436E		7.54	5.79	4.42	0.36
12	81220TN		9.58	9.58	6.96	0.42

BPFI : Ball Passing Frequency on Inner race
 BPFO : Ball Passing Frequency on Outer race
 BSF : Ball Spin Frequency
 FTF : Fundamental Train Frequency

(B-1) Time wave form and power spectrum of AE and Acceleration signal from the point B.

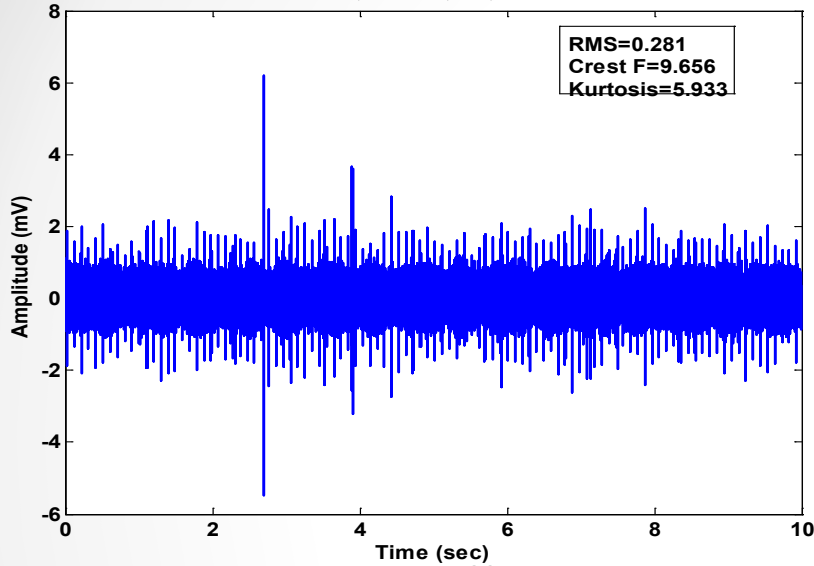


(B-2) Envelope spectrum of AE

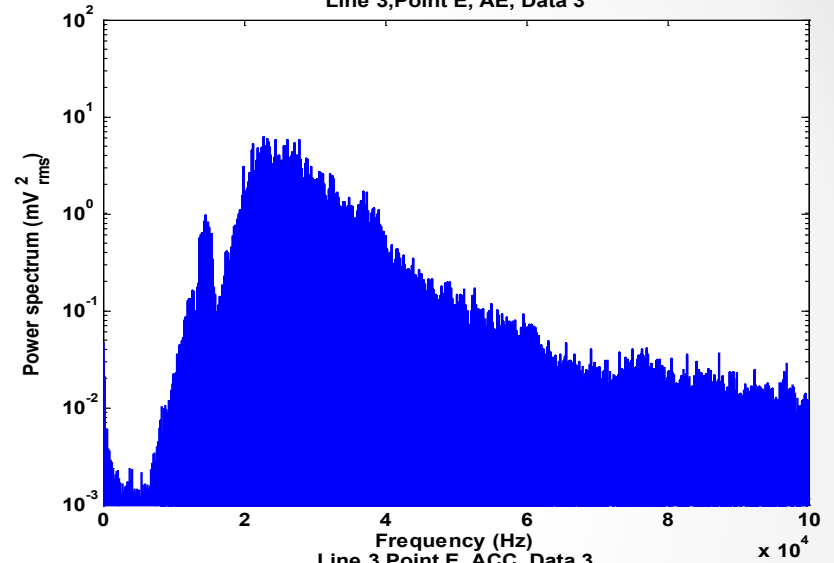


(E-1) Time wave form and power spectrum of AE and Acceleration signal from the point E.

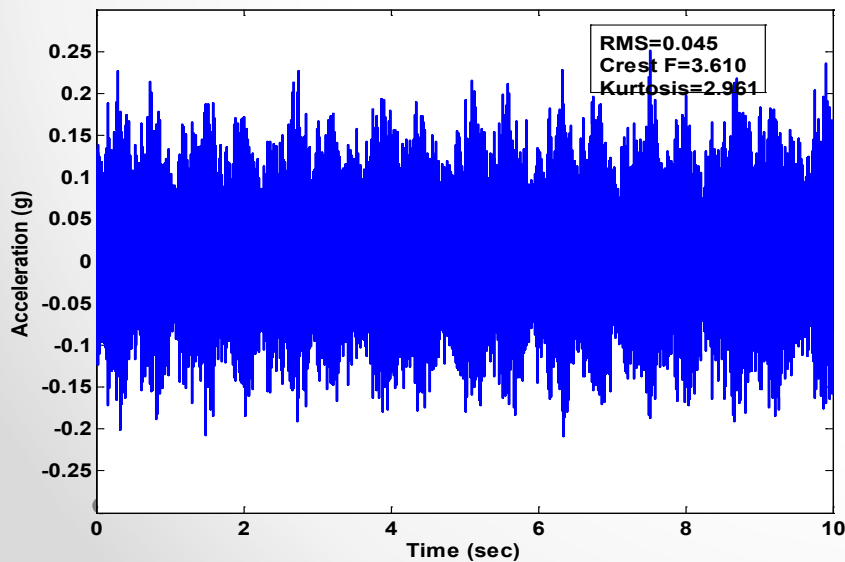
Line3, Point E, AE, Data 3



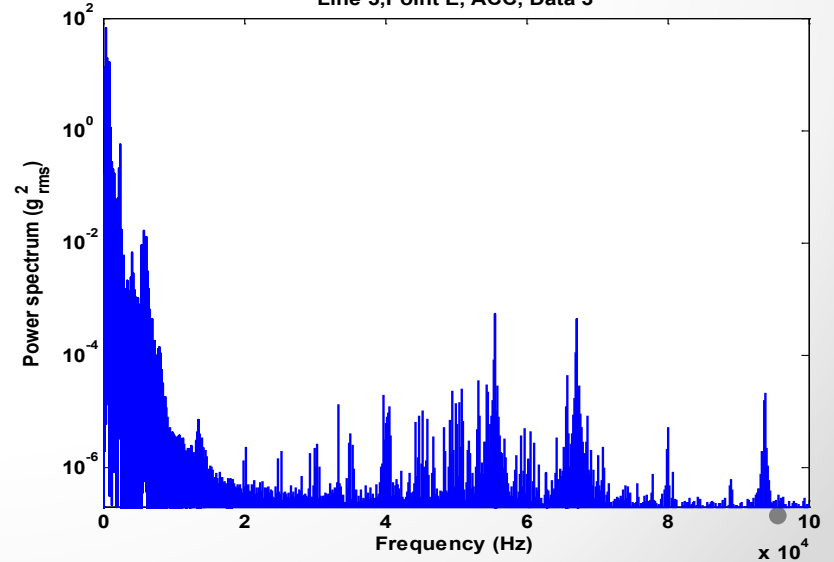
Line 3,Point E, AE, Data 3



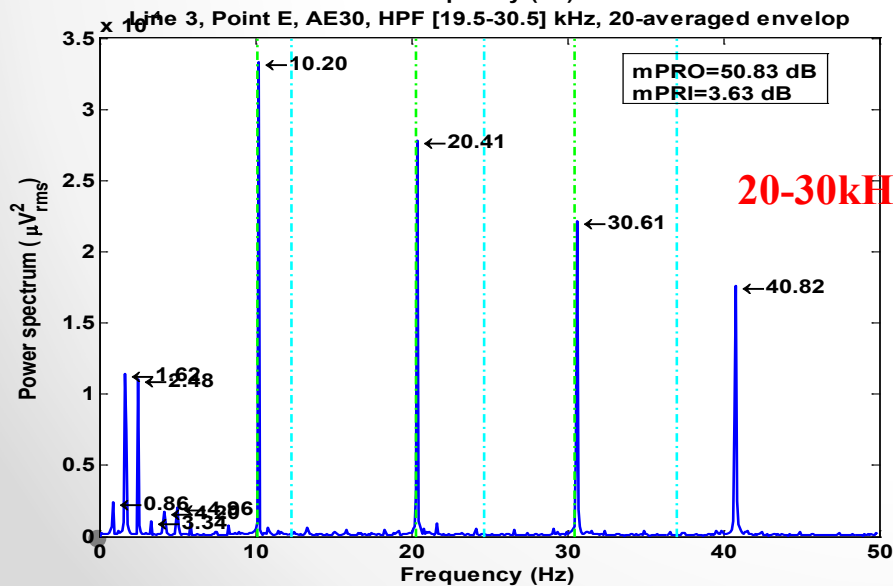
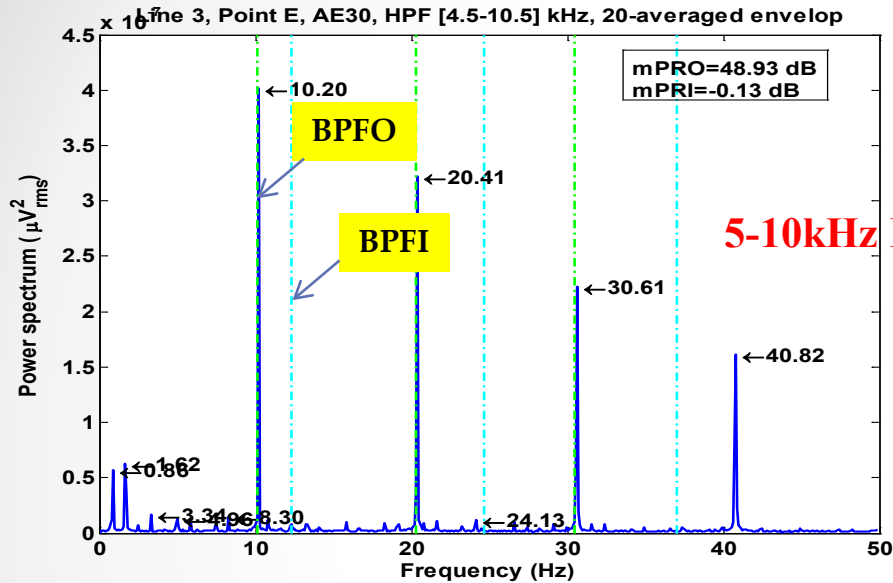
Line3, Point E, ACC, Data 3



Line 3,Point E, ACC, Data 3



(E-2) Envelope spectrum of AE



Observations

- AE energy is distributed within a range of frequency from 10 – 30 kHz, while as the acceleration decreases rapidly after 10 kHz.
- AE signals at points B and E (close to each other) show a series of impulsive impacts occurring at around 10 Hz.
- The enveloped spectrum of point E clearly show the 10 Hz component and its harmonics.
- Point B, close to Point E also detected the 10 Hz component and its harmonics, with smaller amplitudes.
- PHDS has successfully overcome to challenges of high sampling rate and massive data storage.
- Normalisation of multiple AE sensors has provides a clear comparison signal sensitivity and the data are presented in engineering unit rather than just in terms of voltage.

